UDC 593.3 **doi: 10.32620/reks.2026.2.02**

Nataliia UKRAYINETS[1], Tetyana ALYOSHECHKINA[2], Vitaly MIROSHNIKOV[1], Iaroslav GREBENIUK[1], Vladyslav DEMENKO[1], Ihor ARKHYPENKO[1]

[1] National Aerospace University "Kharkiv Aviation Institute", Kharkiv, Ukraine
[2] O. M. Beketov National University of Urban Economy, Kharkiv, Ukraine

STRESS-STRAIN STATE OF A LAYER WITH CYLINDRICAL CAVITIES UNDER SPATIALLY DISTRIBUTED LOADS OF INFINITE EXTENT

The subject of *this article is the stress and strain fields in an isotropic elastic layer in contact with rigid supports and weakened by a system of longitudinal cylindrical cavities. The* ***goal*** *of this study is to mathematically model the stress-strain state of an elastic layer with a specified number of cylindrical cavities; to develop a mathematical model and improve an analytical-numerical approach based on the generalized Fourier method for the exact determination of stress fields in an elastic layer with a specified number of cylindrical cavities under the action of infinitely distributed spatial loads.* ***Tasks****: to formulate a boundary value problem of elasticity theory for a multiconnected layer considering loads that do not decay at infinity; to construct a general solution of the Lamé equation by the superposition method using the auxiliary problem introduction algorithm; to reduce the boundary value problem to solving a quasi-regular infinite system of linear algebraic equations; to perform a numerical analysis for a layer with three cavities and to evaluate the effect of concentrators on stress distribution.* ***The*** *generalized Fourier method is applied to a layer in the Cartesian coordinate system and cavities in local cylindrical coordinate systems. The* ***scientific novelty*** *lies in the creation of an improved approach that combines the generalized Fourier method with the auxiliary problem algorithm. For the first time, the stress distribution and stress concentration patterns in the vicinity of holes for spatially distributed loads acting on an infinite length have been established. This made it possible to obtain the following* ***results****: correctly take into account loads that do not have a periodic structure and do not attenuate at infinity; for an aluminum layer with three cavities, accurate pictures of the distribution of stress tensor components were obtained and zones of their maximum concentration were determined; analysis of the stress state showed that ignoring the mutual influence of cutouts leads to an underestimation of the calculated stresses by more than 20%.* ***Conclusions****: The study's results explain the complex interactions among general layer bending, local deformations, and stress-field interference from neighboring concentrators. The significant asymmetry of the stress state confirms the presence of bending moments, and the rapid attenuation of disturbances is consistent with Saint-Venant's principle. The practical value of the work lies in the potential to use the data obtained to design critical components of aviation technology (integral wing panels, floor power profiles) to increase reliability and reduce weight.*

Keywords*:* *stress-strain state; Lamé equation; generalized Fourier method; layer with cylindrical cavities; spatially distributed loads; analytical and numerical methods.*

1. Introduction

1.1. Motivation

Determining the stress-strain state (SSS) of perforated structures is critical for the aerospace industry, where lightweight systems with high specific stiffness are a priority. The presence of technological cavities reduces weight but simultaneously creates stress concentration areas.

A significant drawback of existing calculation methods is their limited applicability to cases of spatially distributed loads of infinite extent characteristic of real-world operation. This creates a need to improve the mathematical apparatus.

The results obtained will make it possible to improve the accuracy of critical component design (wing panels, turbine blades, etc.), optimize their geometry, and predict their service life. Thus, the development of analytical and numerical methods for assessing the stress-strain state of perforated layers is timely and relevant.

1.2. State of the art

Various approaches are used to analyze the local effects in the area of stress concentrators. For example, in [1], the use of the integral equation method for a half-plane is proposed, which can be adapted for layered structures.

Foreign researchers often focus on related problems using other methodological approaches. The homogenization (averaging) method is effective for the analysis of materials with several periodically arranged voids. This approach allows determining the effective mechanical properties of perforated bodies without a detailed consideration of each void.

In [2], a numerical analysis of the stress-strain state of a tubular shell with preformed holes was performed using an isogeometric approach based on NURBS and T-Splines, which improved the accuracy of the description of geometry and stresses. Study [3] assessed the stability of functionally graded cylindrical shells fixed in an elastic medium under lateral pressure – the dependencies of critical loads on gradience parameters were obtained. Work [4] considers the thermomechanical analysis of composite cylindrical shells with temperature-dependent material properties, enabling more accurate prediction of their behavior under combined thermal and mechanical loading. A mathematical model of the stability of thin transversely gradient shells is presented in [5], which considers the change in material properties across the thickness, which is important for calculating elements with internal cavities. Finally, in [6], the stress state of cylindrical shells with tangential holes-nozzles under the action of internal pressure is investigated, which has direct practical significance for structures with cylindrical cavities in mechanical and power engineering.

In recent years, active research has focused on modeling deformations and stresses in structures subjected to spatially distributed loads. In [7], the dynamic response of beams on a heterogeneous foundation under a moving distributed load was analyzed, which clarified the influence of the foundation parameters and the load shape on the oscillatory characteristics of the system. The approach proposed in [8] uses Chebyshev's spectral approximation to calculate beams with variable properties and loads along their length, providing a universal numerical tool for solving uneven force distribution problems. The loss of stability of plates with elastically fixed edges under the action of an uneven mechanical load around the perimeter was considered in [9], which made it possible to identify critical dependencies on the shape of the force distribution. Higher deformation theories for thin functionally graded shells have been developed [10], describing their static response under various types of distributed loads. Finally, the study [11] demonstrates the effectiveness of the finite element method for analyzing circular porous plates under heterogeneous loads, emphasizing the versatility of modern numerical approaches for complex spatially distributed influences.

As shown in the review [12], modern methods are evolving toward three-dimensional modeling, which allows volumetric deformation effects to be considered.

However, the analysis of publications reveals a significant limitation: most works consider either local effects (one hole) or averaged material properties (many small pores). The case of a spatially infinite load distributed over the surface without a clear periodicity remains outside the attention of researchers. The lack of analytical and numerical-analytical methods adapted to such conditions is a scientific problem, the solution of which is the goal of this work.

Analytical and numerical methods, in particular the generalized Fourier method, are the most effective tools for solving boundary problems of elasticity theory in canonical multiply connected regions. The fundamental principles of which are set out in the monograph by Nikolaev O. G. and Protsenko V. S. [13]. This method allows the boundary conditions on different surfaces to be satisfied with high accuracy.

Significant progress has been made in the application of the generalized Fourier method to problems involving an elastic layer. Miroshnikov et al. investigated the Stress-Strain State (SSS) of a layer with a cylindrical cavity under a periodic load [14] and on a rigid base [15].

The work [16] is devoted to considering spatially infinite loads for a layer with a single cavity.. It is noteworthy that in [16], the results of the analytical solution were verified using the finite element method (FEM), which confirms the validity of the approach used. This makes [16] a benchmark source for verifying the generalization of the proposed system of cavities. In [16], an auxiliary problem was introduced to ensure the correct integration of such loads. However, this approach has not yet been extended to multiple cavities.

Several studies using the generalized Fourier method have been devoted to specific boundary conditions and complex geometry. These include the analysis of non-classical mixed conditions [17], problems with smooth contact, and given displacements [18, 19]. Problems with one elastic inclusion [20], two [21], and contact problems for bodies with many inclusions [22] form a separate direction.

The applied aspects of the method are also being developed: modeling the rotation of a layer with a pipe [23], analyzing the influence of torsional moments on tangential stresses in the coupling of a pipe with a rigid shaft, and calculating bearing connections [24] and cantilever plates with linear supports [25]. A solution for layers with complex combinations of inclusions (pipes and cavities) is obtained in [26].

However, a critical analysis of these sources reveals several unresolved issues:

1. Problem of infinite distributed loads for a body system In [16], the authors proposed an algorithm for introducing an auxiliary problem to correctly account for infinite spatial loads, but this solution was obtained for only one cavity. In works that consider cavity systems [19, 26], the emphasis is on the geometric compo-

nent or periodic influences, ignoring the general distributed loads that do not attenuate at infinity.

2. Lack of comprehensive approach Existing methods are effective for either complex geometry with simple loads or complex loads with simple geometry. The combination of these two factors (domain multi-connectivity and undamped load) remains unaddressed by researchers.

These issues remain unresolved due to the objective complexity of mathematical modeling: standard integral transforms (in particular, Fourier transforms [27]) do not work correctly with functions that do not decay at infinity, and the procedure for their adaptation (regularization) for the case of multiple cavities leads to cumbersome systems of equations that are difficult to solve without specially developed algorithms.

Thus, the problem of determining the SSS of a layer with a system of (several) cylindrical cavities under the action of infinitely distributed spatially distributed loads (which do not have a clear periodic structure and do not decay at infinity) remains open. Solving this problem is the goal of this study.

1.3. Objectives and tasks

This study aims to mathematically model the stress-strain state of an elastic layer with a specified number of cylindrical cavities under the action of infinitely distributed spatial loads. This goal involves developing a mathematical model and improving an analytical-numerical approach based on the generalized Fourier method to determine the stress-strain state of an elastic layer with a specified number of cylindrical cavities subjected to infinitely distributed loads. This will enable reliable data on stress field distributions and account for the mutual influence of concentrators, which is necessary to ensure the reliability and optimization of critical aviation structures.

The structure of the article.

Section 2 discusses the numerical study's materials, methods, simplifications, and assumptions.

Section 3:

1. The boundary value problem of elasticity theory is formulated for a layer weakened by a system of longitudinal cylindrical cavities, considering the action of undamped external loads and support reactions at infinity (subsection 3.1).

2. A general solution to the Lamé equation is constructed by superimposing the basic solutions for the layer and cylinders using an algorithm for introducing an auxiliary problem for the correct integration of infinite spatial loads (subsection 3.2).

3. The boundary conditions on the flat boundaries of the layer and the cylindrical surfaces of the cavities are reduced to solving an infinite system of linear algebraic equations using the addition theorems for basis functions (subsection 3.3). The following equations are obtained.

4. A numerical analysis of the stress state of a layer with three cavities is performed, stress concentration zones are determined, and the influence of the number of these stress concentrators on the distribution of force fields is evaluated by comparison with the case of a single cavity (subsection 3.4).

Section 4 discusses the problem-solving results and the obtained stress state.

Conclusions of the research results are presented in Section 5.

2. Materials and methods of research

The object of this study is the stress-strain state of a linearly elastic isotropic layer weakened by a system of longitudinal cylindrical cavities under the action of infinitely distributed spatially distributed loads and support reactions.

The subject of the research is a mathematical model that describes this state using the analytical-numerical modeling methods.

The main hypothesis of the study is that the application of the generalized Fourier method in combination with the auxiliary problem introduction algorithm will allow us to construct a correct analytical solution for loads that do not decay at infinity and accurately account for the effects of the mutual influence of several stress concentrators.

The following assumptions are made in this study:

1. The structural material is a homogeneous isotropic elastic body.
2. The behavior of the material is described by Hooke's physical linear law.
3. Deformations are considered small, which allows the use of the linear elasticity theory equations.
4. There are no geometric imperfections in the cavity and layer shapes.

Simplifications accepted in the study:

1. An infinite system of linear algebraic equations is solved by the reduction method (by truncating to a finite order), which ensures the specified accuracy of the calculations.
2. A model case of ideal contact or specified stresses is considered without considering the physical nonlinearity of contact with supports.

Theoretical studies are based on the Lamé equilibrium equation in displacements. The generalized Fourier method [13] is used as the main analytical tool. This method involves representing the desired displacement functions as a superposition of the basis solutions of the Lamé equation for a layer (in Cartesian coordinates) and a cylinder (in local cylindrical coordinates):

$$\vec{u}_k^{\pm}(x,y,z;\lambda,\mu)=N_k^{(d)}e^{i(\lambda z+\mu x)\pm\gamma y}; \quad (1)$$

$$\vec{R}_{k,m}(\rho,\varphi,z;\lambda)=N_k^{(p)}I_m(\lambda\rho)e^{i(\lambda z+m\varphi)};$$

$$\vec{S}_{k,m}(\rho,\varphi,z;\lambda)=N_k^{(p)}\left[(\mathrm{sign}\lambda)^m K_m(|\lambda|\rho)\times\right. \quad (2)$$

$$\times e^{i(\lambda z+m\varphi)};\ k=1,2,3;$$

$$N_1^{(d)}=\frac{1}{\lambda}\nabla;\ N_3^{(d)}=\frac{i}{\lambda}\mathrm{rot}\left(\vec{e}_3^{(1)}\right);$$

$$N_2^{(d)}=\frac{4}{\lambda}(\nu-1)\vec{e}_2^{(1)}+\frac{1}{\lambda}\nabla(y);$$

$$N_1^{(p)}=\frac{1}{\lambda}\nabla;\quad N_3^{(p)}=\frac{i}{\lambda}\mathrm{rot}\left(\vec{e}_3^{(2)}\right);$$

$$N_2^{(p)}=\frac{1}{\lambda}\left[\nabla\left(\rho\frac{\partial}{\partial\rho}\right)+4(\nu-1)\left(\nabla-\vec{e}_3^{(2)}\frac{\partial}{\partial z}\right)\right];$$

$$\gamma=\sqrt{\lambda^2+\mu^2},\ -\infty<\lambda,\mu<\infty,$$

where ν is Poisson's ratio; $I_m(\lambda\rho)$, $K_m(|\lambda|\rho)$ are modified Bessel functions of the first and second kind. The functions $\vec{u}_k^{(-)}$ and $\vec{u}_k^{(+)}$ ($k=1,2,3$) are called solutions of the Lamé equation for a layer, and the functions $\vec{R}_{k,m}$, $\vec{S}_{k,m}$ ($k=1,2,3$; $m=0,\pm1,\pm2,...$) are the internal and external solutions of the Lamé equation for a cylinder, respectively. The boundary conditions on different surfaces (flat boundaries of the layer and cylindrical surfaces of cavities) are matched using addition theorems [13]. These transition formulas for basic functions contain modified Bessel and trigonometric functions:

- external solutions for a cylinder $\vec{S}_{k,m}$ can be written in terms of solutions for a layer $\vec{u}_k^{(-)}$ (when $y>0$) and $\vec{u}_k^{(+)}$ (when $y<0$) using the formulas:

$$\vec{S}_{k,m}(\rho,\varphi,z;\lambda)=\frac{(-i)^m}{2}\int_{-\infty}^{\infty}\omega_{\mp}^m\cdot e^{-i\mu\bar{x}_p\pm\gamma\bar{y}_p}\times$$

$$\times\vec{u}_k^{(\mp)}\cdot\frac{d\mu}{\gamma},\quad k=1,\ 3;$$

$$\vec{S}_{2,m}(\rho,\varphi,z;\lambda)=\frac{(-i)^m}{2}\int_{-\infty}^{\infty}\omega_{\mp}^m\cdot\left(\left(\pm m\cdot\mu-\frac{\lambda^2}{\gamma}\pm\right.\right. \quad (3)$$

$$\left.\pm\lambda^2\bar{y}_p\right)\vec{u}_1^{(\mp)}\mp\lambda^2\vec{u}_2^{(\mp)}\pm4\mu(1-\nu)\vec{u}_3^{(\mp)}\Big)\times$$

$$\times\frac{e^{-i\mu\bar{x}_p\pm\gamma\bar{y}_p}d\mu}{\gamma^2},$$

where $\bar{x}_p=\ell_{1p}\cos\alpha_{1p}$, $\bar{y}_p=\ell_{1p}\sin\alpha_{1p}$,

$$\omega_{\mp}(\lambda,\mu)=\frac{\mu\mp\gamma}{\lambda},\ m=0,\pm1,\pm2,\ldots;$$

- the transition from the solutions for the layer $\vec{u}_k^{(+)}$ and $\vec{u}_k^{(-)}$ to the internal solutions for the cylinder $\vec{R}_{k,m}$, can be performed using the following formulas:

$$\vec{u}_k^{(\pm)}(x,y,z)=e^{i\mu\bar{x}_p\pm\gamma\bar{y}_p}\cdot\sum_{m=-\infty}^{\infty}(i\cdot\omega_{\mp})^m\vec{R}_{k,m},$$

$$(k=1,3);$$

$$\vec{u}_2^{(\pm)}(x,y,z)=e^{i\mu\bar{x}_p\pm\gamma\bar{y}_p}\cdot\sum_{m=-\infty}^{\infty}\Big[(i\cdot\omega_{\mp})^m\cdot\lambda^{-2}\times \quad (4)$$

$$\times\left(\left(m\cdot\mu+\lambda^2\bar{y}_p\right)\cdot\vec{R}_{1,m}\pm\gamma\cdot\vec{R}_{2,m}+4\mu(1-\nu)\vec{R}_{3,m}\right)\Big],$$

where $\vec{R}_{k,m}=\vec{\tilde{b}}_{k,m}(\rho,\lambda)\cdot e^{i(m\varphi+\lambda z)}$;

$$\vec{\tilde{b}}_{1,n}(\rho,\lambda)=\vec{e}_\rho\cdot I_n'(\lambda\rho)+i\cdot I_n(\lambda\rho)\cdot\left(\vec{e}_\varphi\frac{n}{\lambda\rho}+\vec{e}_z\right);$$

$$\vec{\tilde{b}}_{2,n}(\rho,\lambda)=\vec{e}_\rho\cdot\left[(4\nu-3)\cdot I_n'(\lambda\rho)+\lambda\rho_p I_n''(\lambda\rho)\right]$$

$$+\vec{e}_\varphi i\cdot m\left(I_n'(\lambda\rho)+\frac{4(\nu-1)}{\lambda\rho}I_n(\lambda\rho)\right)+\vec{e}_z i\lambda\rho I_n'(\lambda\rho);$$

$$\vec{\tilde{b}}_{3,n}(\rho,\lambda)=-\left[\vec{e}_\rho\cdot I_n(\lambda\rho)\frac{n}{\lambda\rho}+\vec{e}_\varphi\cdot i\cdot I_n'(\lambda\rho)\right];$$

$\vec{e}_\rho$, $\vec{e}_\varphi$, $\vec{e}_z$ are unit vectors of the cylindrical coordinate system;

- to transition from solutions for cylinder number p to solutions for cylinder number q, we will use the following formulas:

$$\vec{S}_{k,m}(\rho_p,\varphi_p,z;\lambda)=\sum_{n=-\infty}^{\infty}\vec{b}_{k,pq}^{mn}(\rho_q)\cdot e^{i(n\varphi_q+\lambda z)}, \quad (5)$$

$$k=1,\ 2,\ 3;$$

$$\vec{b}_{1,pq}^{mn}(\rho_q)=(-1)^n\tilde{K}_{m-n}(\lambda\ell_{pq})\cdot e^{i(m-n)\alpha_{pq}}\cdot\vec{\tilde{b}}_{1,n}(\rho_q,\lambda);$$

$$\vec{b}_{2,pq}^{mn}(\rho_q)=(-1)^n\left\{\tilde{K}_{m-n}(\lambda\ell_{pq})\cdot\vec{\tilde{b}}_{2,n}(\rho_q,\lambda)-\frac{\lambda}{2}\ell_{pq}\times\right.$$

$$\left.\times\left[\tilde{K}_{m-n+1}(\lambda\ell_{pq})+\tilde{K}_{m-n-1}(\lambda\ell_{pq})\right]\cdot\vec{\tilde{b}}_{1,n}(\rho_q,\lambda)\right\}\times$$

$$\times e^{i(m-n)\alpha_{pq}};$$

$$\vec{b}_{3,pq}^{mn}(\rho_q)=(-1)^n\tilde{K}_{m-n}(\lambda\ell_{pq})\cdot e^{i(m-n)\alpha_{pq}}\cdot\vec{\tilde{b}}_{3,n}(\rho_q,\lambda);$$

where α_{pq} is the angle between the axis x_p and the segment ℓ_{qp};

$$\tilde{K}_m(x)=(\mathrm{sign}(x))^m\cdot K_m(|x|).$$

The consideration of spatially infinite loads is a distinctive feature of the methodology. The superposition method is used for this purpose. According to this method, the general solution $\vec{U}$ is sought as the sum

$\vec{U} = \vec{U}_0 + \vec{U}_1$. Here, $\vec{U}_0$ is the solution of the auxiliary problem for a solid layer under the action of a given load. This ensures that the conditions at infinity are satisfied. The component $\vec{U}_1$ is a corrective solution for a layer with voids, which ensures that the boundary conditions on the holes' surfaces are satisfied. The developed algorithm was numerically implemented by reducing the boundary value problem to an infinite system of linear algebraic equations of the second kind. The next step was to solve it directly. An aluminum alloy of the Al-Cu-Mg system (grade D16T) was selected for the calculations. The following elastic characteristics were used: Young's modulus $E = 7.1 \cdot 10^{10}$ Pa, Poisson's ratio $\nu = 0.3$.

The developed algorithm was verified by reducing the problem to a special case – a single cylindrical cavity layer. The obtained results were compared with the analytical solution and FEM modeling results from [16]. The results confirm the correctness of the developed methodology and its suitability for generalization to an arbitrary number of cavities

.

3. Results and Discussion

3.1. Mathematical formulation of the boundary value problem for a cavity system layer

In accordance with the first objective of the research, a mathematical model was constructed — a boundary value problem was formulated for an elastic layer (Fig. 1) containing a finite number (N) of parallel cylindrical cavities. The shell is bounded by planes $y = h$ (upper boundary) and $y = -\tilde{h}$ (lower boundary) from the coordinate center and is subjected to surface loads. The radii of these holes are denoted as R_p.

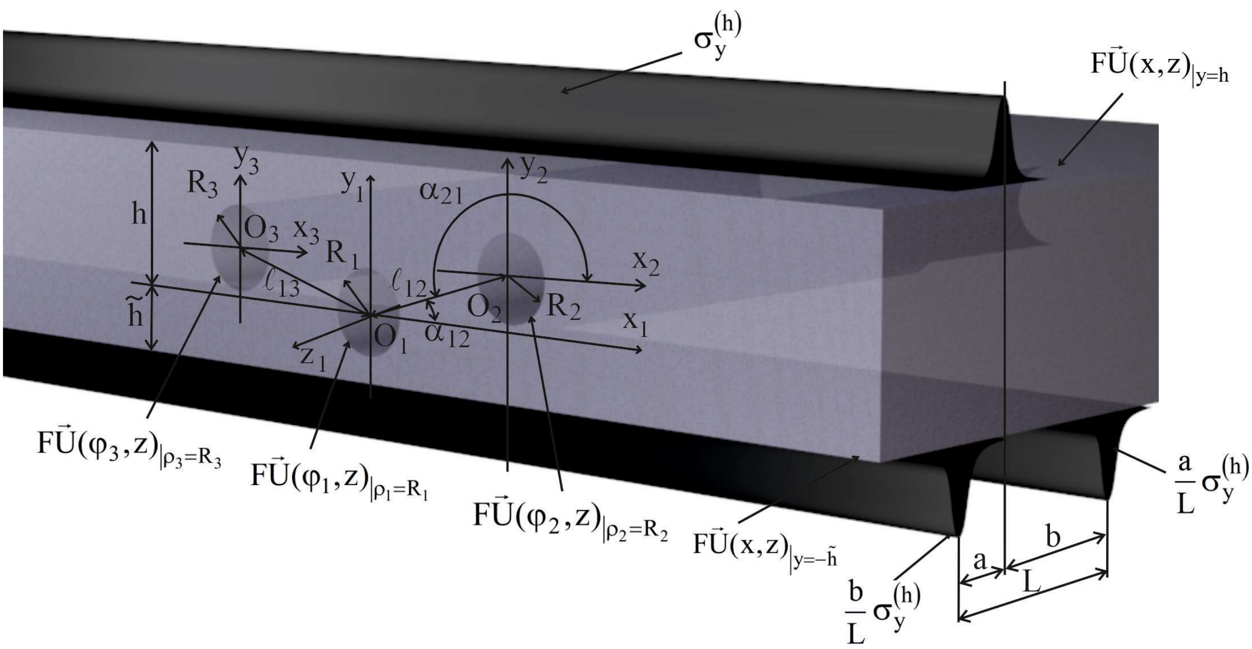

Fig. 1. Layer with cylindrical cavities and infinitely distributed loads

Each cavity (p), its own local cylindrical coordinates (ρ_p, φ_p, z) are used, while the layer itself is described in a general Cartesian system (x, y, z), which coincides and is oriented identically with the coordinate system of the first cavity ($p = 1$).

The solution of the Lamé equation must be determined based on the following boundary conditions:

– at the upper and lower boundaries of the layer, the stresses

$$F\vec{U}(x,z)_{|y=h} = \vec{F}_h^0(x,z),\quad F\vec{U}(x,z)_{|y=-\tilde{h}} = \vec{F}_{\tilde{h}}^0(x,z),$$

where $F\vec{U} = 2 \cdot G \cdot \left[\frac{\sigma}{1 - 2 \cdot \sigma} \vec{n} \cdot \operatorname{div}\vec{U} + \frac{\partial}{\partial n}\vec{U} + \frac{1}{2}\left(\vec{n} \times \operatorname{rot}\vec{U}\right) \right]$ is the stress operator,

$$\begin{aligned} \vec{F}_h^0(x,z) &= \tau_{yx}^{(h)}\vec{e}_x + \sigma_y^{(h)}\vec{e}_y + \tau_{yz}^{(h)}\vec{e}_z, \\ \vec{F}_{\tilde{h}}^0(x,z) &= \tau_{yx}^{(\tilde{h})}\vec{e}_x + \sigma_y^{(\tilde{h})}\vec{e}_y + \tau_{yz}^{(\tilde{h})}\vec{e}_z, \end{aligned} \tag{6}$$

where $\tau_{yx}^{(h)}$, $\sigma_{y}^{(h)}$, $\tau_{yz}^{(h)}$ are constant functions along the *x*-axis;

– stresses are specified on the cavities' surfaces

$$F\vec{U}(\varphi_p, z)\big|_{\rho_p=R_p} = \vec{F}_p^0(\varphi_p, z),$$

where

$$\begin{aligned}
\vec{F}_1^0(\varphi_1, z) &= \sigma_\rho^{(1)}\vec{e}_\rho + \tau_{\rho\varphi}^{(1)}\vec{e}_\varphi + \tau_{\rho z}^{(1)}\vec{e}_z,\\
\vec{F}_2^0(\varphi_2, z) &= \sigma_\rho^{(2)}\vec{e}_\rho + \tau_{\rho\varphi}^{(2)}\vec{e}_\varphi + \tau_{\rho z}^{(2)}\vec{e}_z,\\
\vec{F}_3^0(\varphi_3, z) &= \sigma_\rho^{(3)}\vec{e}_\rho + \tau_{\rho\varphi}^{(3)}\vec{e}_\varphi + \tau_{\rho z}^{(3)}\vec{e}_z.
\end{aligned} \tag{7}$$

Based on the statics conditions, for the elasticity theory problem, the equilibrium equations must be satisfied in the stresses

$$\iint_{(\sigma)} \vec{F}(M)d\sigma = 0, \quad \iint_{(\sigma)} \vec{r}\times\vec{F}(M)d\sigma = 0, \tag{8}$$

where $\sigma = \{\sigma_1 \cup \sigma_2\}$, σ_1 is plane at $y = h$, σ_2 is plane at $y = -\tilde{h}$,

$$\vec{F}(M) = \begin{cases} \vec{F}_h^0(x,z) \text{ на } \sigma_1 \\ \vec{F}_{\tilde{h}}^0(x,z) \text{ на } \sigma_2 \end{cases},$$

$\vec{r}$ is the radius vector of point M.

The specificity of the problem is that the loads do not have a clear periodic structure and do not decay at infinity along the *x*-coordinate, which requires a special approach to constructing the solution.

3.2. Construction of a general solution by superposition

The superposition principle is used to solve the second problem. The general solution of the Lamé equation $\vec{U}$ is presented as the sum of two components:

$$\vec{U} = \vec{U}_0 + \vec{U}_1.$$

$\vec{U}_0$'s problem is auxiliary for considering infinitely distributed loads. It models a layer without an internal cavity, where stress functions corresponding to this load act on the upper boundary and stresses corresponding to support reactions act on the lower boundary. The solution to this problem is as follows:

$$\vec{U}_0 = \sum_{k=1}^{3}\int_{-\infty}^{\infty}\sum_{n=-\infty}^{\infty}\Big(H_{k,n}^{(0)}(\lambda)\cdot\vec{u}_k^{(+)}(x,y,z;\lambda,\mu_n) + \tilde{H}_{k,n}^{(0)}(\lambda)\cdot\vec{u}_k^{(-)}(x,y,z;\lambda,\mu_n)\Big)d\lambda, \tag{9}$$

where $H_{k,n}^{(0)}(\lambda)$ and $\tilde{H}_{k,n}^{(0)}(\lambda)$ are unknowns that must be found from the boundary conditions of this auxiliary problem; $\vec{u}_k^{(+)}(x,y,z;\lambda,\mu_n)$, $\vec{u}_k^{(-)}(x,y,z;\lambda,\mu_n)$ are the basic solutions of Lamé's equation for the layer [13].

To find the unknowns of equation (9), we substitute the known functions $\tau_{yx}^{(h)}$, $\sigma_{y}^{(h)}$, $\tau_{yz}^{(h)}$ into the left side of equation (9), after first expanding them into a Fourier series along the *x*-axis (as constants) and a Fourier integral [26] along the *z*-axis (as rapidly decaying):

$$\vec{F}_h^0(x,z) = \int_{-\infty}^{\infty}\sum_{n=-\infty}^{\infty}\vec{c}_h^{\,0}(\lambda,n)e^{i(\mu_n x+\lambda z)}d\lambda,$$

$$\vec{F}_{\tilde{h}}^0(x,z) = \int_{-\infty}^{\infty}\sum_{n=-\infty}^{\infty}\vec{c}_{\tilde{h}}^{\,0}(\lambda,n)e^{i(\mu_n x+\lambda z)}d\lambda,$$

where

$$\begin{aligned}
\vec{c}_h^{\,0}(\lambda,n) &= \begin{cases} n=0,\ P_h \dfrac{1}{2\pi}\displaystyle\int_{-\infty}^{\infty}\vec{F}_h^0(x,z)e^{-i(\lambda z)}dz \\ \qquad n\neq 0,\ 0 \end{cases},\\
\vec{c}_{\tilde{h}}^{\,0}(\lambda,n) &= \begin{cases} n=0,\ P_{\tilde{h}} \dfrac{1}{2\pi}\displaystyle\int_{-\infty}^{\infty}\vec{F}_{\tilde{h}}^0(x,z)e^{-i(\lambda z)}dz \\ \qquad n\neq 0,\ 0 \end{cases},
\end{aligned} \tag{10}$$

P_h, $P_{\tilde{h}}$ are given constants.

After removing the series, integrals, and the factor $e^{i(\mu_n x+\lambda z)}$ from the right and left sides, we obtain a system of linear algebraic equations for finding $H_{k,n}^{(0)}(\lambda)$, $\tilde{H}_{k,n}^{(0)}(\lambda)$:

$$\begin{cases}
\sum_{s=1}^{3}H_{k,n}^{(0)}(\lambda)\vec{d}_s^{\,+}(h;\lambda,\mu_n) + \\
+\tilde{H}_{k,n}^{(0)}(\lambda)\vec{d}_s^{\,-}(h;\lambda,\mu_n) = \vec{c}_h^{\,0}(\lambda,n), \\
\sum_{s=1}^{3}H_{k,n}^{(0)}(\lambda)\vec{d}_s^{\,+}(-\tilde{h};\lambda,\mu_n) + \\
+\tilde{H}_{k,n}^{(0)}(\lambda)\vec{d}_s^{\,-}(-\tilde{h};\lambda,\mu_n) = \vec{c}_{\tilde{h}}^{\,0}(\lambda,n),
\end{cases} \tag{11}$$

where $\vec{d}_s^{\,\pm}(y;\lambda,\mu_n) = N_k^{(d)}\cdot e^{\pm\gamma y}$.

Equation (11) is projected onto the coordinate axes (equivalent projections at the basis vectors $\vec{e}_x$, $\vec{e}_y$, $\vec{e}_z$) and expressed as integral densities $H_{k,n}^{(0)}(\lambda)$ and $\tilde{H}_{k,n}^{(0)}(\lambda)$:

$$H_{j,n}^{(0)}(\lambda) = \sum_{k=1}^{3}\frac{A_{k,j}}{D}\left(\vec{c}_h^{\,0}(\lambda,n)\right)\vec{e}_k + \sum_{k=1}^{3}\frac{A_{k+3,j}}{D}\left(\vec{c}_{\tilde{h}}^{\,0}(\lambda,n)\right)\vec{e}_k;$$

$$\tilde{H}^{(0)}_{j,n}(\lambda)=\sum_{k=1}^{3}\frac{A_{k,j+3}}{D}\left(\vec{c}^{\,0}_{h}(\lambda,n)\right)\vec{e}_k+$$
$$+\sum_{k=1}^{3}\frac{A_{k+3,j+3}}{D}\left(\vec{c}^{\,0}_{\tilde{h}}(\lambda,n)\right)\vec{e}_k,$$

where $j=1,2,3$; $A_{1..6,1..6}$ and D are cofactors and the determinant of the system of equations, respectively.

After determining the unknown functions $H^{(0)}_{k,n}(\lambda)$ and $\tilde{H}^{(0)}_{k,n}(\lambda)$, we determine the stress at the geometric locations of each of the three cavities. To do this, we use formulas that allow us to move from the basis solutions of the layer ($\vec{u}^{(+)}_k$ and $\vec{u}^{(-)}_k$) to the internal basis solutions of the cylinder ($\vec{R}_{k,m}$) [13].

After removing the integrals over λ and the factor $e^{i(\lambda z+m\varphi)}$, we obtain the stresses at the geometric locations of the three cavities:

$$\sigma^{(1)}_{k,m}(\rho,\lambda)=\sum_{n=-\infty}^{\infty}\left[\sum_{i=1}^{3}\sum_{j=1}^{3}\left(r_{j,k}(R_1;m,\lambda)\cdot f^{(1)}_{i,j}(\lambda,\mu_n,m)\cdot\sum_{t=1}^{3}\frac{A_{t,i}}{D}\left(\vec{c}_h(\lambda,n)\cdot\vec{e}_t\right)\right)+\right.$$
$$\left.+\sum_{i=1}^{3}\sum_{j=1}^{3}\left(r_{j,1}(R_1;m,\lambda)\cdot\tilde{f}^{(1)}_{i,j}(\lambda,\mu_n,m)\cdot\sum_{t=1}^{3}\frac{A_{t,i+3}}{D}\left(\vec{c}_h(\lambda,n)\cdot\vec{e}_t\right)\right)\right],$$

$$\sigma^{(2)}_{k,m}(\rho,\lambda)=\sum_{n=-\infty}^{\infty}\left[\sum_{i=1}^{3}\sum_{j=1}^{3}\left(r_{j,k}(R_2;m,\lambda)\cdot f^{(2)}_{i,j}(\lambda,\mu_n,m)\cdot\sum_{t=1}^{3}\frac{A_{t,i}}{D}\left(\vec{c}_h(\lambda,n)\cdot\vec{e}_t\right)\right)+\right.$$
$$\left.+\sum_{i=1}^{3}\sum_{j=1}^{3}\left(r_{j,1}(R_2;m,\lambda)\cdot\tilde{f}^{(2)}_{i,j}(\lambda,\mu_n,m)\cdot\sum_{t=1}^{3}\frac{A_{t,i+3}}{D}\left(\vec{c}_h(\lambda,n)\cdot\vec{e}_t\right)\right)\right],$$

$$\sigma^{(3)}_{k,m}(\rho,\lambda)=\sum_{n=-\infty}^{\infty}\left[\sum_{i=1}^{3}\sum_{j=1}^{3}\left(r_{j,k}(R_3;m,\lambda)\cdot f^{(3)}_{i,j}(\lambda,\mu_n,m)\cdot\sum_{t=1}^{3}\frac{A_{t,i}}{D}\left(\vec{c}_h(\lambda,n)\cdot\vec{e}_t\right)\right)+\right.$$
$$\left.+\sum_{i=1}^{3}\sum_{j=1}^{3}\left(r_{j,1}(R_3;m,\lambda)\cdot\tilde{f}^{(3)}_{i,j}(\lambda,\mu_n,m)\cdot\sum_{t=1}^{3}\frac{A_{t,i+3}}{D}\left(\vec{c}_h(\lambda,n)\cdot\vec{e}_t\right)\right)\right],$$

$$f^{(1)}_{i,j}(\lambda,\mu,m)=\left(i\cdot\omega_{-}(\lambda,\mu)\right)^m\cdot\begin{pmatrix}1&0&0\\ \frac{m\mu}{\lambda^2}&\frac{\gamma}{\lambda^2}&\frac{4\mu(1-\nu)}{\lambda^2}\\ 0&0&1\end{pmatrix};$$

$$\tilde{f}^{(1)}_{i,j}(\lambda,\mu,m)=\left(i\cdot\omega_{+}(\lambda,\mu)\right)^m\cdot\begin{pmatrix}1&0&0\\ \frac{m\mu}{\lambda^2}&-\frac{\gamma}{\lambda^2}&\frac{4\mu(1-\nu)}{\lambda^2}\\ 0&0&1\end{pmatrix};$$

$$f^{(p)}_{i,j}(\lambda,\mu,m)=\begin{pmatrix}f^{(1)}_{1,1}\cdot e^{i\lambda\bar{x}_p+\gamma\bar{y}_p}&0&0\\ \left(f^{(1)}_{2,1}+\bar{y}_p\cdot f^{(1)}_{1,1}\right)\cdot e^{i\lambda\bar{x}_p+\gamma\bar{y}_p}&f^{(1)}_{2,2}\cdot e^{i\lambda\bar{x}_p+\gamma\bar{y}_p}&f^{(1)}_{2,3}\cdot e^{i\lambda\bar{x}_p+\gamma\bar{y}_p}\\ 0&0&f^{(1)}_{3,3}\cdot e^{i\lambda\bar{x}_p+\gamma\bar{y}_p}\end{pmatrix},\text{ when } p=2,3;$$

$$\tilde{f}^{(p)}_{i,j}(\lambda,\mu,m)=\begin{pmatrix}\tilde{f}^{(1)}_{1,1}\cdot e^{i\lambda\bar{x}_p-\gamma\bar{y}_p}&0&0\\ \left(\tilde{f}^{(1)}_{2,1}+\bar{y}_p\cdot\tilde{f}^{(1)}_{1,1}\right)\cdot e^{i\lambda\bar{x}_p-\gamma\bar{y}_p}&\tilde{f}^{(1)}_{2,2}\cdot e^{i\lambda\bar{x}_p+\gamma\bar{y}_p}&\tilde{f}^{(1)}_{2,3}\cdot e^{i\lambda\bar{x}_p+\gamma\bar{y}_p}\\ 0&0&\tilde{f}^{(1)}_{3,3}\cdot e^{i\lambda\bar{x}_p+\gamma\bar{y}_p}\end{pmatrix},\text{ when } p=2,3;$$

when $k=1$, the stress is considered $\sigma^{(p)}_{\rho}$; when $k=2$, the stress is $\tau^{(p)}_{\rho\varphi}$; when $k=3$, the stress is $\tau^{(p)}_{\rho z}$; $\vec{e}_t$, $t=1,2,3$, is the Cartesian coordinate system;

$r_{j,k}(R;m,\lambda)$ is the tensor obtained by applying the stress operator to $\vec{R}_{k,m}$; the functions $\vec{c}_h(\lambda,n)$ are given in formula (10).

The main task of $\vec{U}_1$ is to model a layer with three cylindrical cavities, on the surface of which stresses $\sigma^{(p)}_{k,m}(\rho,\lambda)$ are acting, taken with opposite signs.

The solution for $\vec{U}_1$ is as follows, according to [22]:

$$\begin{aligned}\vec{U}_1 = &\sum_{k=1}^{3}\int_{-\infty}^{\infty}\int_{-\infty}^{\infty}\Big(H_k(\lambda,\mu)\cdot\vec{u}_k^{(+)}(x,y,z;\lambda,\mu)+\\ &+\tilde{H}_k(\lambda,\mu)\cdot\vec{u}_k^{(-)}(x,y,z;\lambda,\mu)d\mu d\lambda+\\ &+\sum_{p=1}^{3}\sum_{k=1}^{3}\int_{-\infty}^{\infty}\sum_{m=-\infty}^{\infty}B^{(p)}_{k,m}(\lambda)\times\\ &\times\vec{S}_{k,m}\left(\rho_p,\phi_p,z;\lambda\right)d\lambda,\end{aligned} \tag{15}$$

where $\vec{u}_k^{(+)}(x,y,z;\lambda,\mu)$ and $\vec{u}_k^{(-)}(x,y,z;\lambda,\mu)$ are the Lamé equation's based on solutions for layer (2);

$\vec{S}_{k,m}\left(\rho_p,\phi_p,z;\lambda\right)$ Lamé equation's based on solutions outside the cylinder;

$H_k(\lambda,\mu)$, $\tilde{H}_k(\lambda,\mu)$ and $B^{(p)}_{k,m}(\lambda)$ are unknown functions determined from boundary conditions (6) and (7) without the periodic function considered in the auxiliary problem.

The boundary conditions on the surfaces of cylindrical cavities are created by considering stresses (14) with the opposite sign.

3.3. Reducing the boundary value problem to a system of algebraic equations

Equation (15) is written in local coordinate systems using transition formulas between the basis solutions of the Lamé equation [13].

To find the unknown functions of equation (15), a system of 15 integro-algebraic equations was developed.

The boundary conditions on the planes of layer (6) were used to obtain the first six equations. The essence of the process was that the stresses were first calculated (using the operator) for equation (15) and a double Fourier integration was performed for equation (6), and then these expressions were equated. It was also necessary to convert the based on solutions $\vec{S}_{k,m}$ from cylindrical coordinates to Cartesian coordinates via $\vec{u}_k^{(\pm)}$ using formulas (3).

The other 9 equations describe the stress boundary conditions for the three cavities. The obtained stress results (14) were substituted into the left side of Eq. (15), to which the stress operator was previously applied. All basis solutions were first transformed from Cartesian to cylindrical coordinates using formulas (4), and the basis solutions $\vec{S}_{k,m}$ for all other cavities ($q \neq p$) were converted to local cylindrical coordinates using formulas (5).

Using the first six equations, the coefficients $H_k(\lambda,\mu)$ and $\tilde{H}_k(\lambda,\mu)$ were expressed in terms of $B^{(p)}_{k,m}(\lambda)$ and substituted into the other obtained relations. After reducing the series and integrals on both sides of the equality, we obtained an infinite system of nine linear algebraic equations of the second kind. The reduction method was applied to solve it,, which allowed determining the unknown functions $B^{(p)}_{k,m}(\lambda)$. The found values $B^{(p)}_{k,m}(\lambda)$ were used to calculate $H_k(\lambda,\mu)$, $\tilde{H}_k(\lambda,\mu)$.

3.4. Numerical analysis of the stress state of a three-cavity layer

A layer with a height of $h+\tilde{h}=11+11=22$ mm has 3 cylindrical cavities with a radius of $R_p=5$ mm.

The cavities are located on the same horizontal axis ($y=0$), the distance between the centers of the cavities is $\ell_{12}=\ell_{13}=18$ mm, $\alpha_{12}=0$, $\alpha_{13}=\pi$.

The stresses at the layer's upper boundary are given by

$$\sigma_y^{(h)}(x,z)=-10^8\cdot\left(z^2+10^2\right)^{-2},$$
$$\tau_{yx}^{(h)}(x,z)=\tau_{yz}^{(h)}(x,z)=0,$$

at the lower boundary, the support reactions are given in the form of stresses

$$\sigma_y^{(\tilde{h})}(x,z)=\frac{-10^8 b}{\left((z-a)^2+10^2\right)^2 L}-\frac{10^8 a}{\left((z+b)^2+10^2\right)^2 L},$$
$$L=a+b=30+30=60 \text{ mm}.$$

Zero stresses are specified on the cylindrical surfaces of the cavities: $\sigma_\rho^{(p)}=\tau_{\rho\varphi}^{(p)}=\tau_{\rho z}^{(p)}=0$.

The infinite system was limited by order $m=4$. This ensured that the boundary conditions were satisfied with an accuracy of 10^{-4} (or higher) for variable values ranging from 0 to 1.

The numerical implementation of the developed algorithm yielded distributions of the stress tensor components for a layer with three voids. For verification, the developed algorithm was applied to a special case—a layer with a single cavity (N = 1)—under the same geometric and loading parameters. The obtained results agreed with the analytical solution and the FEM calculation presented in [16]. This confirms the algorithm's accuracy; after which it was applied to the main configuration.

Stresses arise at the upper and lower boundaries of the layer under the influence of the specified loads and support reactions, as shown in Fig. 2.

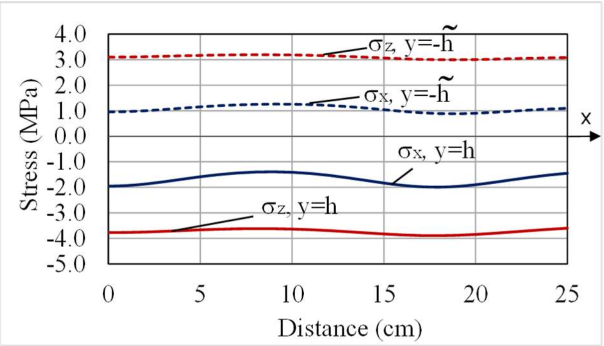

Fig. 2. Stresses σ_x and σ_z at the upper ($y = h$) and lower ($y = -\tilde{h}$) boundaries of the layer along the x-axis

Fig. 2 shows that the external load causes significant disturbances in the stress state in the cavity projection areas. The significant asymmetry of the stress distribution relative to the median plane is a characteristic feature, which confirms the presence of combined bending and tensile-compressive deformation. The maximum values of normal stresses on the surfaces occur in the load application zones and above the axis of each cavity.

Fig. 3 shows the distribution of normal stresses σ_x , σ_z and the applied load σ_y at the upper boundary of the layer along the longitudinal axis *z*. Here, the solid lines correspond to the calculation scheme with three cavities, and the dotted lines correspond to the case with one cavity, the results of which were verified using the FEM method in [16].

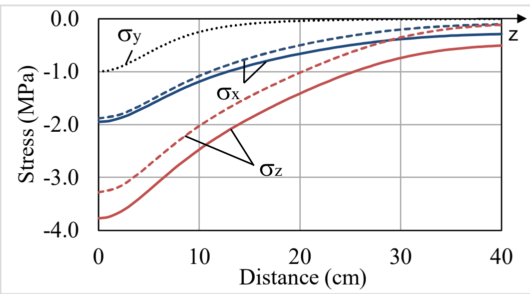

Fig. 3. Stresses at the upper boundary of the layer ($y = h$) along the *z*-axis

Localized stress is observed in the load application zone ($z = 0$). The maximum stress values at this point are $\sigma_x = -1.95094$ MPa, $\sigma_z = -3.77148$ MPa. When moving away from the load center along the *z*-axis, the stress amplitudes σ_x and σ_z show rapid attenuation, approaching zero values at a distance slightly exceeding the distance to the support ($b = 30$ mm). This behavior is fully consistent with Saint-Venant principle, according to which localized force factors form local stress fields.

The amplitude values of stresses σ_z (red line) for a system with three holes exceed the corresponding values for a single hole by approximately 13%. This indicates that ignoring adjacent notches in calculations leads to an underestimation of the actual compressive stresses.

Fig. 4 shows the corresponding stress distributions at the lower edge of the layer ($y = -\tilde{h}$) along the *z*-axis. The dotted lines indicate the lines used to calculate a layer with a single cavity.

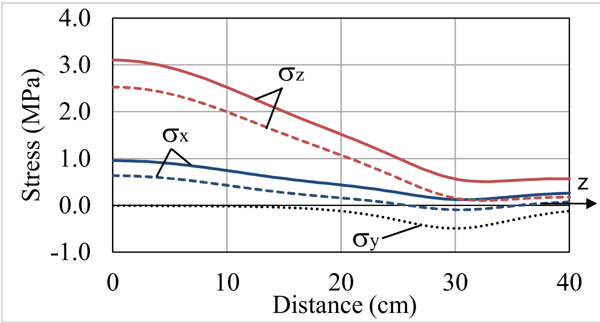

Fig. 4. Stresses at the lower edge of the layer ($y = -\tilde{h}$)

The stress distribution at the lower edge differs from that at the upper edge in both magnitude and the nature of the change, due to the influence of support reactions and the presence of cutouts. The maximum stress values at $z = 0$ at this point are $\sigma_x = 0.955317$ MPa, $\sigma_z = 3.103655$ MPa. Local stress fluctuations are recorded at the support location. A comparison of Fig. 3 and Fig. 4 further illustrates the unevenness of the stress state across the thickness of the perforated layer.

The difference between solid lines (3 cavities) and dotted lines (1 cavity) is even more pronounced here. The maximum stress σ_z for a system with three cavities reaches 3.103655 MPa, whereas it is 2.52635 MPa for a single cavity. This increase in stress (over 22%) is explained by a decrease in the cross-section’s effective stiffness and a redistribution of force flows to the bridges between the holes.

Fig. 5 shows a detailed analysis of the stress state directly in the stress concentrator zone, which shows the distribution of normal stresses on the surface of the first cylindrical cavity ($p=1$).

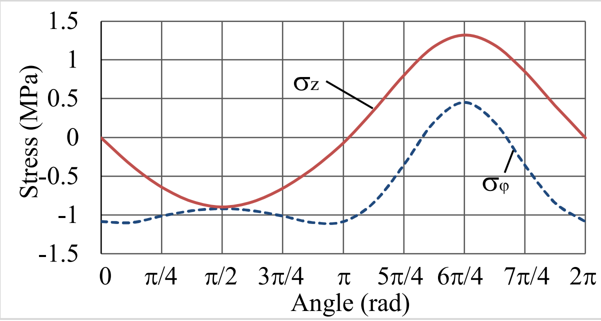

Fig. 5. Stress on the cylindrical cavity surface $p=1$ at $z=0$

The stress distribution along the angular coordinate φ has a complex oscillatory character. The stresses σ_φ show a clearly pronounced periodicity with maxima at $\varphi \approx 0^\circ$ and $\varphi \approx 180^\circ$, which corresponds to the cavity's horizontal diameter. The maximum compressive stresses are equal to $\sigma_\varphi = -1.1005$ MPa, and the tensile stresses are $\sigma_\varphi = 0.45231$ MPa. These values exceed the applied external load (–1 MPa), confirming the effect of stress concentration near the cylindrical hole.

The stress distribution σ_z shows a clear dependence: compression occurs in the upper zone of the cavity (at $\varphi \approx 90^\circ$ $\sigma_z = -0.89792$ MPa) and stretching occurs in the lower zone of the cavity (at $\varphi \approx 270^\circ$ $\sigma_z = 1.31863$ MPa).

The obtained results of the mathematical and numerical modeling and the analytical derivations are explained by the physical nature of the interaction of force fields in multiply connected domains and the chosen mathematical model's correctness. The proposed approach demonstrates that modeling based on the generalized Fourier method allows for an adequate reproduction of the actual stress state of the structure.

The result of solving the first and second problems of Section 3 (construction of a general solution, formulas (9) and (15)) is explained by applying the superposition principle. The introduction of an auxiliary problem ($\vec{U}_0$) made it possible to analytically describe the stress field from a load that does not attenuate at infinity, and the main problem ($\vec{U}_1$) corrected this field to satisfy the conditions on the surfaces of the cavities.

The reduction to a system of algebraic equations (the third problem in Section 3) was made possible by the basic functions and the use of addition theorems (3) – (5), which ensured the accurate "stitching" of solutions in different coordinate systems.

The asymmetry of the stress fields (relative to the *x*-axis) revealed in the solution of the fourth task (Fig. 2) is explained by the occurrence of internal bending moments relative to the *z*-axis due to the difference in boundary conditions on the upper (load) and lower (support) edges.

The localization of stresses and their rapid attenuation along the *z*-axis (Fig. 3) is a direct manifestation of Saint-Venant's principle: at a distance exceeding the characteristic size of the load application zone (in this case, the distance to the support $b=30$ mm), the influence of local forces is neutralized.

The increase in stress concentration in the model with three holes compared to one (difference of 13–22%, Figs. 3, 4) is explained by the interference of stress fields from neighboring concentrators and a decrease in the bridges' effective cross-section (stiffness).

The oscillatory nature of the stresses on the hole contour (Fig. 5) is explained by the redistribution of force flows that bend around the cavities, creating compression (upper part) and tension (lower zone) zones.

The proposed approach has several advantages over known methods due to the analytical nature of the solution and the ability to accurately satisfy boundary conditions:

1. Unlike works based on the classical finite element method (FEM), where accuracy depends on the mesh density, the result obtained allows the calculation of the stress at any point with a controlled error (in this work, 10^{-4}) without the need to reconfigure the model. This is made possible by the use of accurate Lamé equation basis solutions.

2. Unlike studies that considered periodic loads or local influences, this result allows the analysis of a layer under the action of spatially infinite loads of a general form. This is achieved by introducing the component $\vec{U}_0$ (formula 9) into the solution structure, which integrates undamped loads.

3. Verification of the proposed approach by reducing it to the special case N = 1 demonstrated its agreement with the analytical and FEM solutions presented in [16]. Compared with that work, the result obtained here generalizes the method to the case of an arbitrary cavity system (N cylinders). This made it possible to identify the effects of mutual influence (a 22% increase in stresses) that cannot be estimated within the framework of a single hole model.

The solutions obtained fully address the problem identified in Section 2. The problem was the lack of methods for calculating multiply connected layered bodies under loads that do not decay at infinity. Thanks to the development of an algorithm combining an auxiliary task (to account for the load specifics) and a generalized Fourier method (to account for complex geometry), a closed solution that correctly describes the SSS of such a system was constructed.

When applying the results obtained in practice, the following limitations should be considered:

1. Geometric: the model assumes that the cavities are circular cylinders parallel to each other and to the layer boundaries (their surfaces do not intersect).
2. Physical: the material is considered to be perfectly elastic and isotropic (this is true for metals in the elastic range, but not for composites or plastic deformations).
3. Boundary conditions: contact with supports is modeled through stress distribution (reactions), without considering friction or separation of the layer from the support.

The disadvantages include the method's high mathematical complexity, which requires the calculation of special functions (Bessel functions). When the number of cavities increases or they approach the boundaries of the layer, solving large systems of equations is necessary (requires an increase in the order of reduction m). In addition, the model in this formulation does not consider possible temperature effects.

Further development of this research may involve adapting the method for thermoelasticity and dynamics problems. This is relevant because real aircraft structures (turbine blades, skin) operate under changing temperatures and vibrations. Extending the approach to layers with reinforced holes (inclusions) or holes of other shapes is also promising, which will bring the calculation scheme closer to real engineering structures.

5. Conclusions

The main contribution of this work concerns the modeling methods: a generalization of the analytical-numerical Fourier method combined with the auxiliary problem algorithm is proposed, which for the first time makes it possible to model, in a closed analytical form, the stress-strain state of a multiply connected elastic layer with an arbitrary number of cylindrical cavities under the action of spatially infinite, non-periodic, non-attenuating distributed loads. The developed method removes the limitations of classical integral transforms for functions that do not decay at infinity, ensures the exact satisfaction of the boundary conditions on all surfaces, and reduces the boundary value problem to a quasi-regular infinite system of linear algebraic equations of the second kind, thereby guaranteeing the stability of the computational process and providing a solution of analytical accuracy that purely numerical methods (FEM) cannot achieve.

1. A mathematical model was constructed, and the boundary value problem of elasticity theory was modeled for an isotropic layer weakened by an arbitrary number of longitudinal cylindrical cavities. A distinctive feature of the developed model is the consideration of infinitely distributed spatially distributed loads that do not attenuate at infinity and have no periodic structure. This made it possible to extend the scope of application of calculation schemes to a wider class of real loads that previously could not be accurately analyzed using classical approaches.
2. The superposition method was used to construct a general solution to the Lamé equation, which combines the generalized Fourier method with the auxiliary problem introduction algorithm. This solution structure ($\vec{U} = \vec{U}_0 + \vec{U}_1$) made it possible to analytically consider the non-attenuating load component and ensure the fulfillment of conditions at infinity. This solves the problem of incorrect integral transformations for non-attenuating functions and provides an accurate description of displacement fields both in the concentrator zone and at a distance from them.
3. An effective computational algorithm that reduces the fulfillment of boundary conditions on flat boundaries of the layer and curved surfaces of cavities to the solution of a quasi-regular infinite system of linear algebraic equations of the second kind has been developed. The application of addition theorems for basis functions ensured the exact satisfaction of boundary conditions at all surfaces points. This approach guarantees the stability of the computational process and allows high accuracy in obtaining results (the error does not exceed 10^{-4} when truncating the system).
4. Numerically established stress distribution patterns in an aluminum layer with three cavities. Significant asymmetry of stress fields and a significant influence of concentrator interaction have been revealed: the maximum compressive stresses in the system with three holes exceed the corresponding values for a single hole by 13% at the upper boundary and by more than 22% at the lower boundary of the layer. This is explained by the effects of stress interference and a decrease in the stiffness of the bridges, confirming the need to use multi-link models when designing critical structures.
5. The developed algorithm was verified by reducing the problem to the special case of a single cavity (N = 1). The results obtained are consistent with the analytical solution and the FEM calculation [16], confirming the validity of the proposed approach and its generalization to a system of N cavities

Contributions of authors: Conceptualization, Methodology, Formal Analysis, Writing – Draft Prepa-

ration – **Nataliia Ukrayinets.** Conceptualization, Methodology, Investigation, Writing – Draft Preparation – **Tatyana Alyoshechkina.** Review, Supervision, Project Administration, Writing – Draft Preparation – **Vitaly Miroshnikov.** Software, Data Curation – **Iaroslav Grebeniuk.** Software, Review – **Vladislav Demenko.** Resources, Visualization – **Ihor Arkhipenko**.

All authors have read and approved the final manuscript for publication.

Conflict of interest

The authors declare that they have no conflict of interest with respect to this study, including financial, personal, authorship, or other conflicts that could influence the study and its results presented in this article.

Financing

The study was conducted without financial support.

Data availability

The manuscript has no associated data.

Use of artificial intelligence

The authors confirm that they did not use artificial intelligence technologies in the creation of the presented work.

References

1. Maksymovych, O. V., & Solyar, T. Ya. Determination of stress concentration near dies, holes, and cracks in the half plane based on the method of integral equations and Green solutions. *Journal of Mathematical Sciences*, 2022, vol. 261, no. 2, pp. 162–175. DOI: 10.1007/s10958-022-05745-8.
2. El Fakkoussi, S., Koubaiti, O., Elkhalfi, A., Vlase, S., & Marin, M. Numerical analysis of the cylindrical shell pipe with preformed holes subjected to a compressive load using non-uniform rational B-splines and T-splines for an isogeometric analysis approach. *Mathematics*, 2024, vol. 13, no. 8, pp. 529. DOI: 10.3390/axioms13080529.
3. Ertunç, K., Dilmac, H., & Sofiyev, A. H. Investigation of stability behaviour of clamped functionally graded cylindrical shells in elastic medium under lateral pressure. *Journal of Engineering and Applied Sciences (JEAS)*, 2025, vol. 5, no. 1, pp. 5–15. DOI: 10.61640/ujeas.2025.0501.
4. Li, J., Qian, H., & Lu, C. Thermo-mechanical analysis for composite cylindrical shells with temperature-dependent material properties under combined thermal and mechanical loading. *Materials*, 2025, vol. 18, no. 7, pp. 1391. DOI: 10.3390/ma18071391.
5. Tomczyk, B., Gołąbczak, M., Kubacka, E., & Bagdasaryan, V. Mathematical modeling of stability problems for thin transversally graded cylindrical shells. *Continuum Mech. Thermodyn.*, 2024, vol. 36, pp. 1661–1684. DOI: 10.1007/s00161-024-01322-3.
6. Zhao, X., Qian, C., & Wu, Z. Strength analysis of cylindrical shells with tangential nozzles under internal pressure. *Applied Sciences*, 2024, vol. 14, no. 6, pp. 2363. DOI: 10.3390/app14062363.
7. Huang, Y., Liu, H., & Zhao, Y. Dynamic analysis of non-uniform functionally graded beams on inhomogeneous foundations subjected to moving distributed loads. *Applied Sciences*, 2023, vol. 13, no. 18, pp. 10309. DOI: 10.3390/app131810309.
8. Liu, H., Huang, Y., & Zhao, Y. A unified numerical approach to the dynamics of beams with longitudinally varying cross-sections, materials, foundations, and loads using Chebyshev spectral approximation. *Aerospace*, 2023, vol. 10, no. 10, pp. 842. DOI: 10.3390/aerospace10100842.
9. Wang, C., & Liu, Q. Buckling behaviour of rectangular and skew plates with elastically restrained edges under non-uniform mechanical edge loading. *PLoS ONE*, 2024, vol. 19, no. 9, pp. e0308245. DOI: 10.1371/journal.pone.0308245.
10. Shinde, B. M., Sayyad, A. S., & Naik, N. S. Assessment of a new higher-order shear and normal deformation theory for the static response of functionally graded shallow shells. *Curved and Layered Structures*, 2024, vol. 11, no. 1, pp. 20240014. DOI: 10.1515/cls-2024-0014.
11. Doori, S. G. M., Noori, A. R., & Etemadi, A. Static response of functionally graded porous circular plates via finite element method. *Arabian Journal for Science and Engineering*, 2024, vol. 49, pp. 14167–14181. DOI: 10.1007/s13369-024-08914-w.
12. Liu, H., Deng, L., & Wang, W. 3D stress concentration around circular hole under remote biaxial loading. *International Journal of Mechanical Sciences*, 2024, vol. 268, pp. 109032. DOI: 10.1016/j.ijmecsci.2024.109032.
13. Nikolaev, A. G., & Protsenko, V. S. Generalized Fourier method in spatial problems of the theory of elasticity. Kharkiv: National Aerospace University named after M. Ye. Zhukovsky "KHAI" Publ., 2011, 344 p.
14. Miroshnikov, V., Younis, B., Savin, O., & Sobol, V. A linear elasticity theory to analyze the stress state of an infinite layer with a cylindrical cavity under periodic load. *Computation*, 2022, vol. 10, no. 9, pp. 160. DOI: 10.3390/computation10090160.
15. Miroshnikov, V. Yu. Stress state of an elastic layer with a cylindrical cavity on a rigid foundation. *International Applied Mechanics*, 2020, vol. 56, no. 3, pp. 372–381. DOI: 10.1007/s10778-020-01021-x.
16. Ukrayinets, N., Alyoshechkina, T., Miroshnikov, V., Savin, O., Younis, B., Vynohradov, V., & Murahovska, O. Consideration of spatially infinite loads in the problem for a layer with a cylindrical cavity and continuous supports. *Computation*, 2025, vol. 13, no. 11, pp. 270. DOI: 10.3390/computation13110270.
17. Grebenikov, M. M., & Mironov, K. V. Stress state analysis of a layer with a longitudinal cavity and given non-classical mixed boundary conditions. *Science, Theory and Practice: Proceedings of the 29th*

International Scientific and Practical Conference, Tokyo, Japan, 2021, pp. 536–540. DOI: 10.46299/ISG.2021.I.XXIX.

18. Nikichanov, V. V. Determination of the stress state of a layer with a cylindrical cavity under given smooth contact conditions on the layer boundaries and displacements on the cavity surface. *Scientific Collection "InterConf": Proceedings of the 9th International Scientific and Practical Conference "Scientific Horizon in the Context of Social Crises"*, Tokyo, Japan, 2021, pp. 208–213. Available at: https://ojs.ukrlogos.in.ua/index.php/interconf/issue/view/6-8.08.2021/569 (accessed 6 January 2026).

19. Ilin, O., Kosenko, M., & Denshchykov, O. Analysis of the stress state of a reinforced layer with two cylindrical cavities and some contact-type conditions. *Colloquium-Journal*, 2024, vol. 19, pp. 8–13. DOI: 10.5281/zenodo.12723815.

20. Miroshnikov, V. Yu., Medvedeva, A. V., & Oleshkevich, S. V. Determination of the stress state of the layer with a cylindrical elastic inclusion. *International Conference on Actual Problems of Engineering Mechanics, Materials Science Forum*, 2019, vol. 968, pp. 413–420. DOI: 10.4028/www.scientific.net/MSF.968.413.

21. Miroshnikov, V., Savin, O., Younis, B., & Nikichanov, V. Solution of the problem of the theory of elasticity and analysis of the stress state of a fibrous composite layer under the action of transverse compressive forces. *Eastern-European Journal of Enterprise Technologies*, 2022, vol. 4, no. 7 (118), pp. 23–30. DOI: 10.15587/1729-4061.2022.263460.

22. Ilin, O., & Kosenko, M. Solving the problem of elasticity theory for a ball with a circular inclusion and a circular cavity under given boundary conditions of contact type. *Proceedings of the XXVIII International Scientific and Practical Conference "Development of Science in the Conditions of Deepening European Integration Processes"*, Rome, Italy, 2024, pp. 162–165. Available at: https://eu-conf.com/en/events/development-of-science-in-the-conditions-of-deepening-european-integration-processes/ (accessed 6 January 2026).

23. Vitaly, M. Rotation of the layer with the cylindrical pipe around the rigid cylinder. *Advances in Mechanical and Power Engineering (CAMPE 2021), Lecture Notes in Mechanical Engineering*, Cham: Springer, 2023, pp. 314–322. DOI: 10.1007/978-3-031-18487-1_32.

24. Sverdlov, S. Determination of the stress-strain state of a bearing connection. *Modern Trends in the Development of Economy, Technology and Industry: Collection of Scientific Papers "International Scientific Unity", Proceedings of the 2nd International Scientific and Practical Conference*, Toronto, Canada, 2025, pp. 229–233. Available at: https://isu-conference.com/en/archive/modern-trends-in-the-development-of-economy-technology-and-industry-12-02-25/ (accessed 6 January 2026).

25. Sverdlov, S. Yu. Analysis of the stress-strain state of a cantilever plate with a linear bearing connection. *Open Information and Computer Integrated Technologies*, 2025, no. 104, pp. 82–96. DOI: 10.32620/oikit.2025.104.06.

26. Denshchykov, O. Y. First main problem of the theory of elasticity for a layer with two thick-walled pipes and one cylindrical cavity. *J. Mech. Eng. Mash.*, 2025, vol. 28, pp. 44–53. DOI: 10.15407/pmach2025.02.044.

27. Singh, P., Gupta, A., & Joshi, S. D. General parameterized Fourier transform: A unified framework for the Fourier, Laplace, Mellin and Z transforms. *IEEE Transactions on Signal Processing*, 2022, vol. 70, pp. 1295–1309. DOI: 10.1109/TSP.2022.3152607

Received 09.01.2026, Received in revised form 27.04.2026
Accepted date 10.07.2026, Published date 31.07.2026

НАПРУЖЕНО-ДЕФОРМОВАНИЙ СТАН ШАРУ З ЦИЛІНДРИЧНИМИ ПОРОЖНИНАМИ ПІД ДІЄЮ ПРОСТОРОВО РОЗПОДІЛЕНИХ НАВАНТАЖЕНЬ НЕСКІНЧЕНОЇ ДОВЖИНИ

Н. А. Українець, Т. М. Альошечкіна, В. Ю. Мірошніков, Я. В. Гребенюк, В. Ф. Деменко, І. О. Архипенко

Предметом вивчення статті *є процеси формування напружено-деформованого стану в ізотропному пружному шарі, що контактує з жорсткими опорами та послаблений системою поздовжніх циліндричних порожнин.* ***Метою є*** *математичне моделювання напружено-деформованого стану пружного шару із заданою кількістю циліндричних порожнин, яке полягає у розробці математичної моделі та вдосконаленні аналітико-чисельного підходу на основі узагальненого методу Фур'є для точного визначення полів напружень у пружному шарі із заданою кількістю циліндричних порожнин під дією просторово нескінченних розподілених навантажень.* ***Завдання****: сформулювати граничну задачу теорії пружності для багатозв'язного шару з урахуванням незатухаючих на нескінченності навантажень; побудувати загальний розв'язок рівняння Ламе методом суперпозиції, використовуючи алгоритм введення допоміжної задачі; звести граничну задачу до розв'язання квазірегулярної нескінченної системи лінійних алгебраїчних рівнянь; провести чисельний аналіз для шару з трьома порожнинами та оцінити вплив взаємодії концентраторів на розподіл напружень. Використовуваним* ***методом*** *є Узагальнений метод Фур'є, що застосований до шару в* *декартовій системі координат та порожнин в локальних циліндричних системах координат.* ***Наукова новизна*** *полягає у створенні вдосконаленого підходу, який поєднує узагальнений метод Фур'є з алгоритмом допоміжної задачі, вперше встановлено закономірності розподілу напружень та концентрації напружень в околі отворів для випадку просторово розподілених навантажень, що діють на нескінченній довжині. Це дало можливість отримані такі* ***результати****: коректно врахувати навантаження, які не мають періодичної структури та не затухають на нескінченності; для алюмінієвого шару із трьома порожнинами отримано точні картини розподілу компонент тензора напружень та визначено зони їх максимальної концентрації; аналіз напруженого стану показав, що ігнорування взаємного впливу вирізів призводить до заниження розрахункових напружень на понад 20%.* ***Висновки****: результати дослідження пояснюють складну взаємодію ефектів загального згину шару, локальних деформацій та інтерференції полів напружень від сусідніх концентраторів. Виявлена значна асиметрія напруженого стану підтверджує наявність згинальних моментів, а швидке затухання збурень узгоджується з принципом Сен-Венана. Практична цінність роботи полягає в можливості використання отриманих даних під час проєктування відповідальних елементів авіаційної техніки (інтегральних панелей крила, силових профілів підлоги) для підвищення їх надійності та вагової оптимізації.*

Ключові слова*: напружено-деформований стан; рівняння Ламе; узагальнений метод Фур'є; шар з циліндричними порожнинами; просторово розподілені навантаження; аналітико-чисельні методи.*

Українець Наталія Анатоліївна – ст. викладач каф. вищої математики та системного аналізу, Національний аерокосмічний університет «Харківський авіаційний інститут», Харків, Україна.

Альошечкіна Тетяна Миколаївна – ст. викладач каф. теоретичної і будівельної механіки, Харківський національний університет міського господарства імені О.М. Бекетова, Харків, Україна.

Мірошніков Віталій Юрійович – д-р техн. наук, проф., зав. каф. міцності літальних апаратів, Національний аерокосмічний університет «Харківський авіаційний інститут», Харків, Україна.

Гребенюк Ярослав Володимирович – канд. техн. наук, ст. викладач каф. міцності літальних апаратів, Національний аерокосмічний університет «Харківський авіаційний інститут», Харків, Україна.

Деменко Владислав Федорович – канд. техн. наук, доц., проф. каф. міцності літальних апаратів, Національний аерокосмічний університет «Харківський авіаційний інститут», Харків, Україна.

Архипенко Ігор Олексійович – аспірант каф. міцності літальних апаратів, Національний аерокосмічний університет «Харківський авіаційний інститут», Харків, Україна.

Nataliia Ukrayinets – Senior Lecturer at the Department of Higher Mathematics and Systems Analysis, National Aerospace University "Kharkiv Aviation Institute", Kharkiv, Ukraine,
e-mail: n.ukrayinets@khai.edu, ORCID: 0000-0001-7406-5809, Scopus Author ID: 57223964123.

Tetyana Alyoshechkina – Senior Lecturer at the Department of Theoretical and Structural Mechanics, O.M. Beketov National University of Urban Economy in Kharkiv, Kharkiv, Ukraine,
e-mail: Tetiana.Aloshechkina@kname.edu.ua, ORCID: 0000-0001-7234-1558, Scopus Author ID: 57195071162.

Vitaly Miroshnikov – Doctor of Technical Sciences, Professor, Head of the Department of Aircraft Strength, National Aerospace University "Kharkiv Aviation Institute", Kharkiv, Ukraine,
e-mail: v.miroshnikov@khai.edu, ORCID: 0000-0002-9491-0181, Scopus Author ID: 57203680484.

Iaroslav Grebeniuk – Candidate of Technical Science, Senior Lecturer at the Department of Aircraft Strength, National Aerospace University "Kharkiv Aviation Institute", Kharkiv, Ukraine,
e-mail: i.grebeniuk@khai.edu, ORCID: 0009-0004-6032-7125, Scopus Author ID: 59344828300.

Vladyslav Demenko – Candidate of Technical Science, Associate Professor, Professor at the Department of Aircraft Strength, National Aerospace University "Kharkiv Aviation Institute", Kharkiv, Ukraine,
e-mail: v.demenko@khai.edu, ORCID: 0000-0002-9555-4596, Scopus Author ID: 6603516730.

Ihor Arkhypenko – PhD student, the Department of Aircraft Strength, National Aerospace University "Kharkiv Aviation Institute", Kharkiv, Ukraine,
e-mail: i.o.arkhypenko@khai.edu, ORCID: 0009-0009-0311-4437.